

## Electronic Supplementary Information

### **Donor-acceptor Covalent Organic Framework/g-C<sub>3</sub>N<sub>4</sub> Hybrids for Enhanced Visible Light Photocatalytic H<sub>2</sub> Production**

Chenxiang Lin,<sup>a</sup> Chaozheng Han,<sup>a</sup> Lei Gong,<sup>a</sup> Xin Chen,<sup>a</sup> Jinxia Deng,<sup>a</sup> Dongdong

Qi,<sup>a</sup> Yongzhong Bian,<sup>a</sup> Kang Wang,<sup>a</sup> and Jianzhuang Jiang<sup>ab</sup>

<sup>a</sup> *Beijing Key Laboratory for Science and Application of Functional Molecular and Crystalline Materials, Department of Chemistry, School of Chemistry and Biological Engineering, and Daxing Research Institute, University of Science and Technology Beijing, Beijing 100083, China*

<sup>b</sup> *Beijing Advanced Innovation Center for Materials Genome Engineering, University of Science and Technology Beijing, Beijing 100083, China.*

## List of Tables and Figures

- 1** Experimental section.
- 2** Fig. S1 The photocatalytic H<sub>2</sub> evolution activity of x-TBTA/g-C<sub>3</sub>N<sub>4</sub> (x = 0, 1.0, 2.5, 5.0, 7.5, 10.0, 100).
- 3** Fig. S2 TEM images of (a) 1.0-TBTA/g-C<sub>3</sub>N<sub>4</sub>. (b) 5.0-TBTA/g-C<sub>3</sub>N<sub>4</sub>. (c) 7.5-TBTA/g-C<sub>3</sub>N<sub>4</sub> and (d) 10.0-TBTA/g-C<sub>3</sub>N<sub>4</sub>.
- 4** Fig. S3 FTIR spectra of TBTA, 2.5-TBTA/C<sub>3</sub>N<sub>4</sub>, and g-C<sub>3</sub>N<sub>4</sub>.
- 5** Fig. S4 FTIR spectra of as-synthesized samples.
- 6** Fig. S5 The UV-vis diffuse reflectance absorption spectra (DRS) of samples.
- 7** Table S1. Absorption spectroscopic data and energy levels.
- 8** Fig. S6 (a) MS plots of 2.5-TBTA/g-C<sub>3</sub>N<sub>4</sub> and (b) Energy levels of TBTA, 2.5-TBTA/g-C<sub>3</sub>N<sub>4</sub> and g-C<sub>3</sub>N<sub>4</sub>.
- 9** Fig. S7 (a) The photocatalytic H<sub>2</sub> evolution activity with different catalyst amounts of 10-TBTA/g-C<sub>3</sub>N<sub>4</sub>. (b) The photocatalytic H<sub>2</sub> evolution activity with different sacrificial reagents of TBTA. (c) Time dependent photocatalytic H<sub>2</sub> production with AA as asacrificial reagents. (d) Long-term stability for H<sub>2</sub> production of 2.5-TBTA/g-C<sub>3</sub>N<sub>4</sub>-Pt.
- 10** Fig. S8 (a) The photocatalytic H<sub>2</sub> evolution rate of 2.5-TBTA/g-C<sub>3</sub>N<sub>4</sub> with monochromatic light irradiations. (b) Wavelength-dependent photocatalytic H<sub>2</sub> evolution rate and DRS spectrum of 2.5-TBTA/g-C<sub>3</sub>N<sub>4</sub>.
- 11** Table S2. Comparison of the performance of photocatalytic H<sub>2</sub> evolution rate of organic semiconductor/g-C<sub>3</sub>N<sub>4</sub> hybrids with Pt as co-catalysts.

- 12** Table S3. Comparison of the performance of photocatalytic H<sub>2</sub> evolution rate of g-C<sub>3</sub>N<sub>4</sub>-based heterostructured photocatalysts without noble metal as co-catalyst.
- 13** Fig. S9 Comparison of (a) DRS (b) IR before and after H<sub>2</sub> production process.
- 14** Fig. S10 Comparison of TEM images before and after H<sub>2</sub> production process.
- 15** Fig. S11 Elemental mappings of 2.5-TBTA/g-C<sub>3</sub>N<sub>4</sub> after H<sub>2</sub> production process.
- 16** Table S4. PL Decay parameters of samples.
- 17** Notes and references.

## Experimental Section

### Materials

2,4,6-triformylphloroglucinol (TP) and 4,4'-(benzo[c][1,2,5]thiadiazole-4,7-diyl)dianiline (BTDA) were purchased from Jilin Chinese Academy of Sciences-Yanshen Technology Co. Ltd. Chloroplatinic acid, 1,3,5-Trimethylbenzene, 1,4-dioxane, triethanolamine (TEOA), and ascorbic acid were obtained from Saan Chemical Technology Ltd. Urea and methanol was obtained from Sinopharm Chemical Reagent Company, Ltd. All commercial chemicals were used without further purification unless otherwise mentioned.

### Characterizations

Powder X-ray diffraction (PXRD) data were collected on a TTR III multi-function X-ray diffractometer operated at 40 kV and 300 mA with Cu K $\alpha$  radiation. FT-IR spectra were recorded as KBr pellets using a Bruker Tensor 37 spectrometer with 2 cm<sup>-1</sup> resolution. The transmission electron microscopy (TEM) was acquired on HITACHI HT7700 with an electron acceleration energy of 100 kV. The images of high angle annular dark-field scanning transmission electron microscope (HAADF-STEM) and energy dispersive spectroscopy (EDS) mapping were observed by a JEM-ARM200F electron microscope operated at 200 kV. X-ray photoelectron spectroscopy (XPS) data were collected on an ESCALAB 250Xi system. Al K $\alpha$  X-ray (6 mA  $\times$  12 KV) was utilized as the irradiation source. All measurements were performed in the CAE mode with the reference of C 1s (284.80 eV). UV-vis diffuse reflectance

absorption spectra (DRS) were recorded on a Shimadzu UV-2600 UV-vis-NIR spectrophotometer with BaSO<sub>4</sub> as the reference. Steady-state PL spectra (excitation at 500 nm) were measured with a Hitachi F-4500 fluorescence spectrophotometer. Time-resolved photoluminescence spectra (TRPS) were obtained on an Edinburgh FLS 980 fluorescence spectrophotometer with excitation and detection wavelengths of 475 and 615 nm, respectively. Platinum contents were determined using inductively coupled plasma optical emission spectrometer (ICP-OES) with an Agilent ICP-OES 725 ES system, by digesting the hybrids in HNO<sub>3</sub>/HCl (1:3, v/v).

### **Electrochemical measurement**

Photoelectrochemical measurements were conducted on a CHI760E electrochemical workstation in a three-electrode cell. The counter electrode was a Pt wire, and the reference electrode was a Ag/AgCl electrode. For the preparation of the working electrodes, the as-synthesized 4 mg samples were added into a mixed solution of 10  $\mu$ L Nafion and 200  $\mu$ L ethanol, then the catalyst suspension (10  $\mu$ L  $\times$  3) were dropped onto the ITO glass (0.7 cm  $\times$  0.7 cm) surface, forming a film after drying naturally for 12 h. An aqueous solution containing 0.2 M Na<sub>2</sub>SO<sub>4</sub> was used as the electrolyte. The i-t measurements were performed with the light on and off conditions (300 W Xe-lamp,  $\lambda > 420$  nm). The electrochemical impedance spectroscopy (EIS) was performed in the frequency range from 10<sup>-1</sup> to 10<sup>5</sup> Hz with a bias potential of +1.5 V. The Mott-Schottky plots were obtained with a bias potential that ranged from -1.6 to 1.0 V (vs Ag/AgCl) under the frequency of 1000, 1500, and 2000 Hz, respectively.<sup>1,2</sup>

### **Synthesis of g-C<sub>3</sub>N<sub>4</sub> and C<sub>3</sub>N<sub>4</sub>-Pt**

g-C<sub>3</sub>N<sub>4</sub> was prepared according to a reported procedure.<sup>3</sup> C<sub>3</sub>N<sub>4</sub>-Pt was synthesized as follows:<sup>3</sup> g-C<sub>3</sub>N<sub>4</sub> (0.6 g) was added to a mixed solvent of 150 mL deionized water and 60 mL methanol, and then ultrasonically dispersed for 5 min. After adding 1.2 mL of H<sub>2</sub>PtCl<sub>6</sub> solution (0.0386 M in water) under stirring, the resultant suspension was irradiated for 3 h under a 300 W mercury lamp. After being cooled to room temperature, the product was separated by centrifugation and washed with water and EtOH, then dried at 70 °C overnight. The Pt content was 2.08% as determined by ICP-OES.

### **Synthesis of polymer TBTA**

A Pyrex tube (10 mL) was charged with 2,4,6-triformylphloroglucinol (TP) (10.5 mg, 0.05 mmol), 4,4'-(benzo[c][1,2,5]thiadiazole-4,7-diyl)dianiline (BTDA) (24 mg, 0.075 mmol), mesitylene (0.6 mL), and ethanol (2.4 mL). The mixture was sonicated for 1 min, subsequently, 0.3 mL of acetic acid was added. The tube was flash frozen at 77 K using a liquid N<sub>2</sub> bath and degassed by three freeze-pump-thaw cycles, sealed under vacuum and then heated at 120 °C for 3 days. The red precipitate was collected by centrifugation and washed with 1,4-dioxane and anhydrous acetone. After drying at 50 °C for 24 h, the product was obtained as dark red powder (26 mg, 82.7%).

### **Synthesis of x-TBTA/g-C<sub>3</sub>N<sub>4</sub> and 2.5-TBTA/g-C<sub>3</sub>N<sub>4</sub>-Pt (x refers to wt% of TBTA).**

200 mg of g-C<sub>3</sub>N<sub>4</sub> was dispersed in 4.5 mL of mesitylene/ethanol (4:1) in a Pyrex

tube by ultrasonication for 10 min. Subsequently, TP (1.7 mg, 0.008 mmol) and BTDA (3.8 mg, 0.012 mmol) were added and the mixture was sonicated for 5 min. Then, 0.15 mL of acetic acid was added. The tube was flash frozen at 77 K using a liquid N<sub>2</sub> bath and degassed by three freeze-pump-thaw cycles, sealed under vacuum and then heated at 120 °C for 3 days. The light red color precipitate was collected by centrifugation and washed with mesitylene and anhydrous acetone. After drying at 50 °C for 24 h, 2.5-TBTA/g-C<sub>3</sub>N<sub>4</sub> was obtained as light red color powder (185 mg, 92.5%). Following the synthesis procedure of 2.5-TBTA/g-C<sub>3</sub>N<sub>4</sub> with 0.0032 mmol TP and 0.0048 mmol BTDA, 0.016 mmol TP and 0.024 mmol BTDA, 0.024 mmol TP and 0.036 mmol BTDA, and 0.032 mmol TP and 0.048 mmol BTDA instead of 0.008 mmol TP and 0.012 mmol BTDA, respectively, as starting materials, 1.0-TBTA/g-C<sub>3</sub>N<sub>4</sub>, 5.0-TBTA/g-C<sub>3</sub>N<sub>4</sub>, 7.5-TBTA/g-C<sub>3</sub>N<sub>4</sub>, and 10.0-TBTA/g-C<sub>3</sub>N<sub>4</sub> were prepared. In addition, 2.5-TBTA/g-C<sub>3</sub>N<sub>4</sub>-Pt was also prepared by using the synthesis procedure of 2.5-TBTA/g-C<sub>3</sub>N<sub>4</sub> with g-C<sub>3</sub>N<sub>4</sub>-Pt instead of g-C<sub>3</sub>N<sub>4</sub> as the starting material.

### **General procedure for photocatalytic hydrogen evolution**

The measurements were performed in a gas-closed circulation system (AuLight, Beijing, China, CEL-SPH2N). A Xe-lamp (CEL-HXF300, 300 W) equipped with  $\lambda \geq 420$  nm cutoff filter was used as visible-light source, and the temperature was maintained at 5°C using a homoeothermic cooling circulation pump. The H<sub>2</sub> evolution rate was quantified by an online gas chromatograph (GC7980, TCD detector, 13X molecular sieve columns, and Ar carrier). Typically, the photocatalysts (5 mg) was

dispersed in 20 mL deionized water with 0.1 M ascorbic acid as a sacrificial reagent. Before measurement, the reactor was sonicated for 5 min to obtain well-distributed suspension and then illuminated by  $\lambda \geq 420$  nm light from its top after being thoroughly degassed.

### **Density functional theory computational methodology**

The present first principle DFT calculations were performed by Vienna Ab initio Simulation Package (VASP)<sup>5</sup> with the projector augmented wave (PAW) method.<sup>6</sup> The exchange-functional was treated using the generalized gradient approximation (GGA) of Perdew-Burke-Ernzerhof (PBE)<sup>5</sup> functional. The cut-off energy of the plane-wave basis was set at 450 eV for the calculations of atoms and cell optimization. The vacuum spacing in a direction perpendicular to the plane of the catalyst was at least 15 Å. The Brillouin zone integration was performed using 3×3×1 Monkhorst-Pack k-point sampling for a primitive cell.<sup>7</sup> The self-consistent calculations apply a convergence energy threshold of 10<sup>-5</sup> eV. The equilibrium lattice constants were optimized with maximum stress on each atom within 0.05 eV/Å. Finally, the interface adhesion energy ( $E_{\text{ads}}$ ) has been calculated as:  $E_{\text{ads}} = E_{\text{total}} - E_{\text{TBTA}} - E_{\text{g-C}_3\text{N}_4}$ , where  $E_{\text{total}}$  is the energy of TBTA/g-C<sub>3</sub>N<sub>4</sub>,  $E_{\text{TBTA}}$  is the energy of TBTA,  $E_{\text{g-C}_3\text{N}_4}$  is the energy of g-C<sub>3</sub>N<sub>4</sub>.



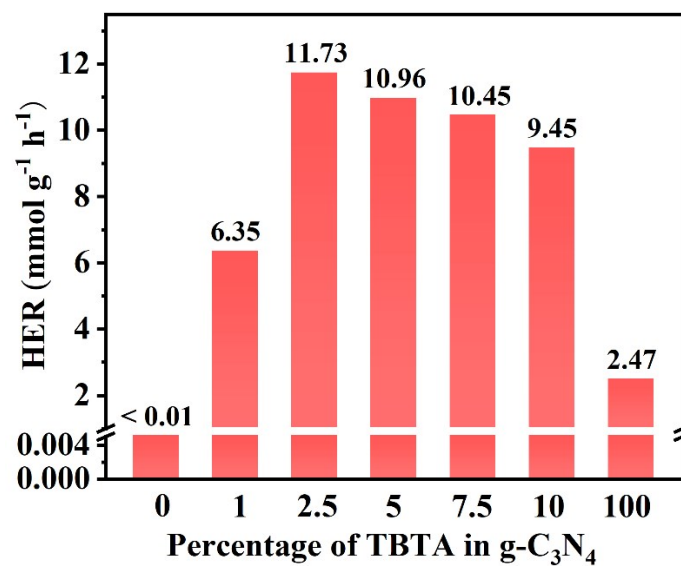


**Fig. S1** The photocatalytic H<sub>2</sub> evolution activity of x-TBTA/g-C<sub>3</sub>N<sub>4</sub> (x = 0, 1.0, 2.5, 5.0, 7.5, 10.0, 100). Note: 5.0 mg catalyst and 20.0 mL deionized water under  $\lambda \geq 420$  nm light irradiation.

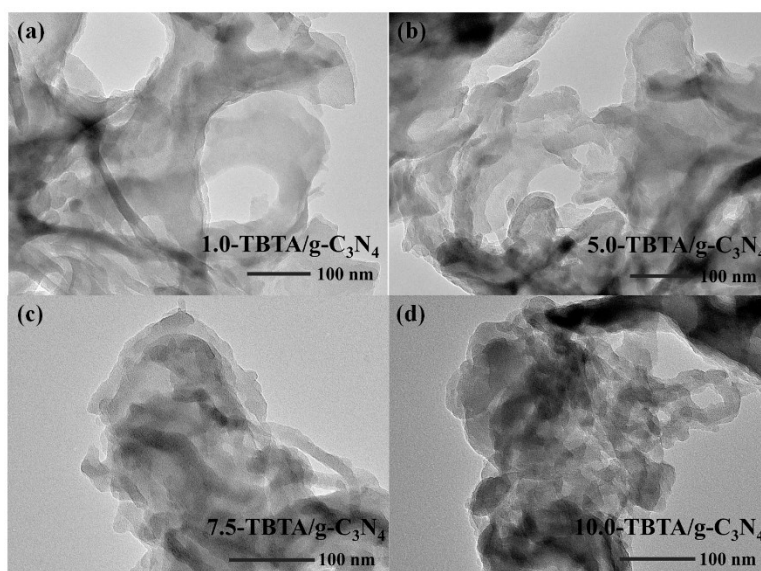


**Fig. S2** TEM images of (a) 1.0-TBTA/g-C<sub>3</sub>N<sub>4</sub>. (b) 5.0-TBTA/g-C<sub>3</sub>N<sub>4</sub>. (c) 7.5-TBTA/g-C<sub>3</sub>N<sub>4</sub> and (d) 10.0-TBTA/g-C<sub>3</sub>N<sub>4</sub>.

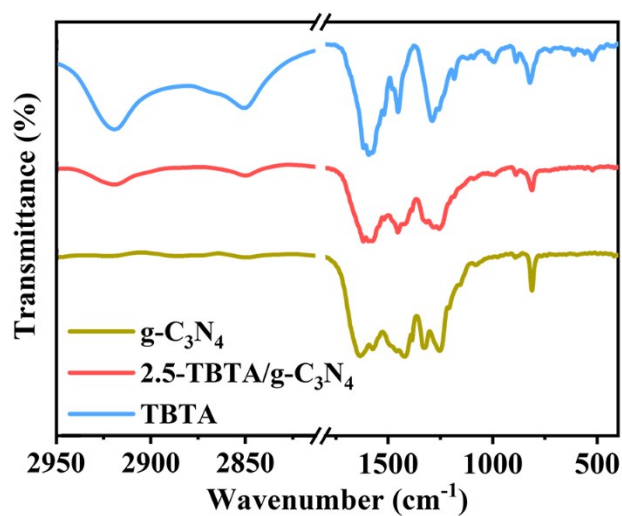


Fig. S3 FTIR spectra of TBTA, 2.5-TBTA/C<sub>3</sub>N<sub>4</sub>, and g-C<sub>3</sub>N<sub>4</sub>.

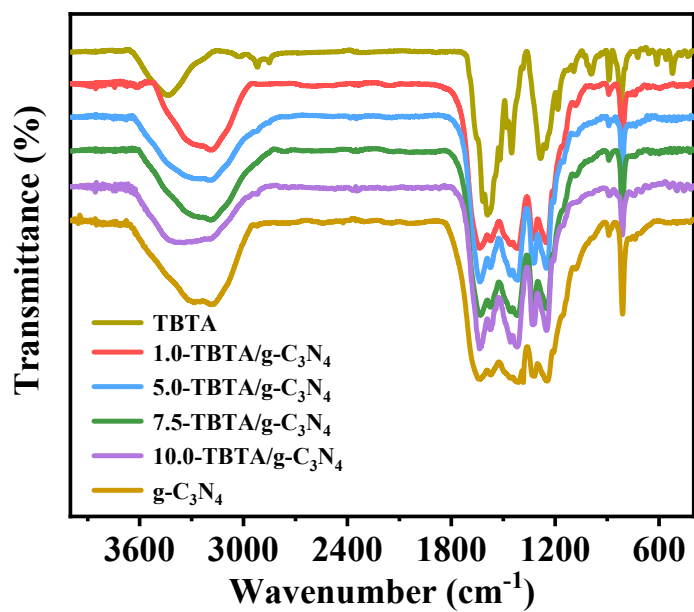
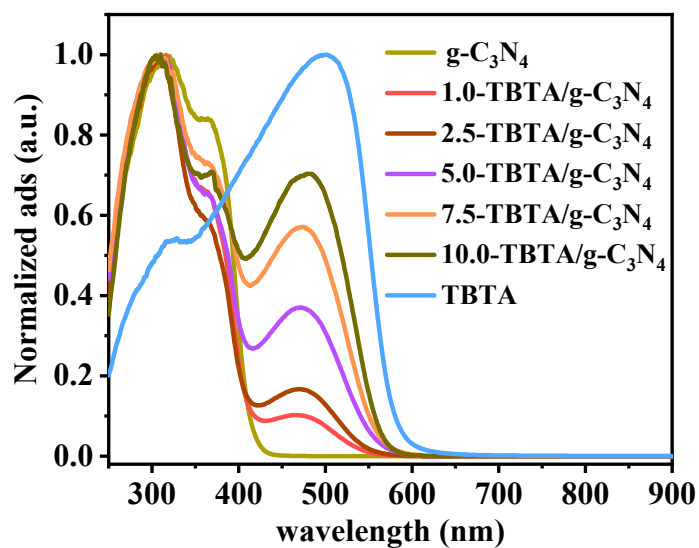


Fig. S4 FTIR spectra of as-synthesized samples.



**Fig. S5** The UV-vis diffuse reflectance absorption spectra (DRS) of samples.

**Table S1.** Absorption spectroscopic data and energy levels.

Sample	$\lambda_{\text{abs-onset}}^a$ (nm)	$E_{\text{CB}}^b$ (V)	$E_{\text{VB}}^c$ (V)	$E_g^d$ (V)
g-C <sub>3</sub> N <sub>4</sub>	428	-1.26	1.64	2.90
TBTA	576	-1.45	0.70	2.15
2.5-TBTA/g-C <sub>3</sub> N <sub>4</sub>	538	-1.265	1.04	2.30

<sup>a</sup> Absorption onset. <sup>b</sup> Determined from Mott-Schottky plots. <sup>c</sup>  $E_{\text{VB}} = E_g + E_{\text{CB}}$ . <sup>d</sup> Determined by the absorption onset from DRS spectra:  $E_g = 1240/\lambda_{\text{abs-onset}}$ .

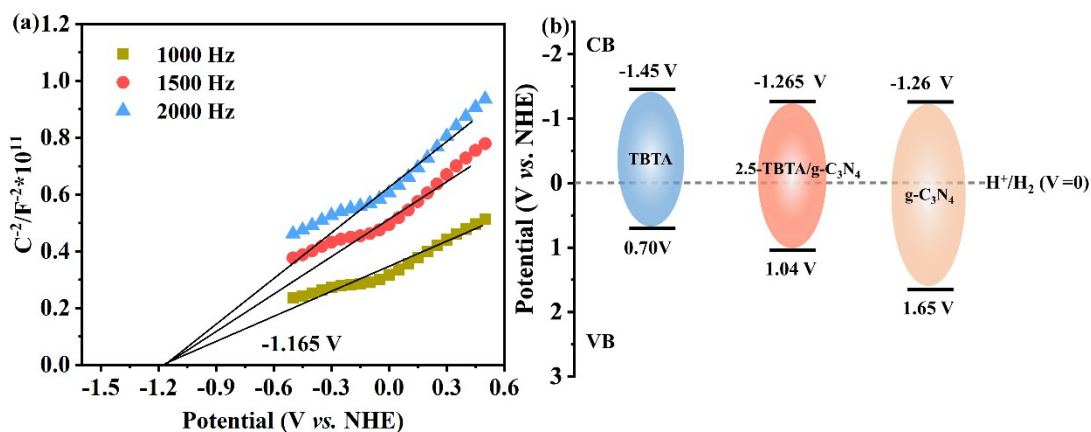


**Fig. S6** (a) MS plots of 2.5-TBTA/g-C<sub>3</sub>N<sub>4</sub> and (b) Energy levels of TBTA, 2.5-TBTA/g-C<sub>3</sub>N<sub>4</sub> and g-C<sub>3</sub>N<sub>4</sub>.

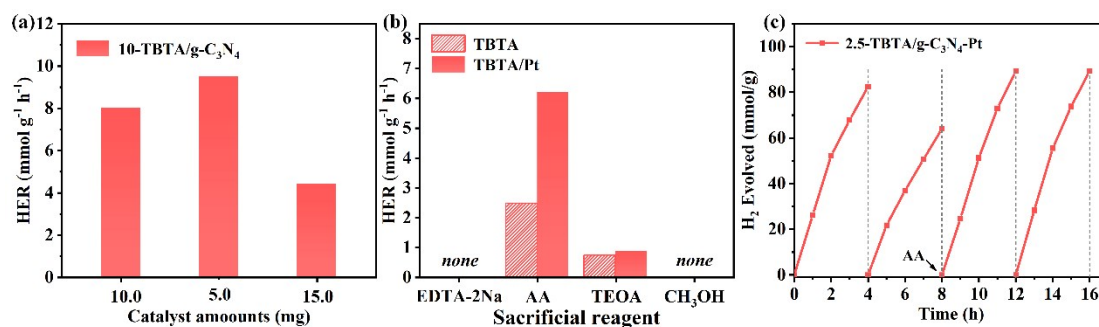


**Fig. S7** (a) The photocatalytic H<sub>2</sub> evolution activity with different catalyst amounts of 10-TBTA/g-C<sub>3</sub>N<sub>4</sub>. (b) The photocatalytic H<sub>2</sub> evolution activity with different sacrificial reagents of TBTA. (c) Long-term stability for H<sub>2</sub> production of 2.5-TBTA/g-C<sub>3</sub>N<sub>4</sub>-Pt. Note: 5.0 mg catalyst and 20.0 mL deionized water under  $\lambda \geq 420$  nm light irradiation.

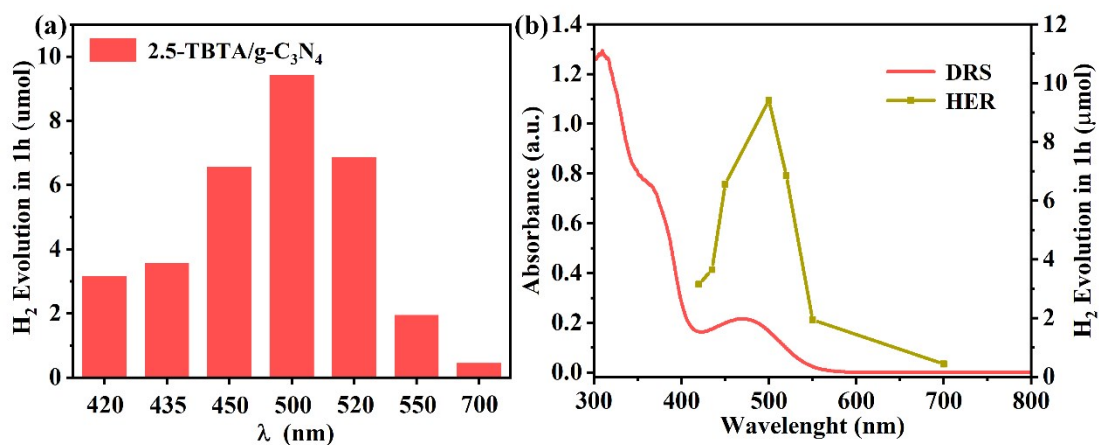


**Fig. S8** (a) The photocatalytic H<sub>2</sub> evolution rate of 2.5-TBTA/g-C<sub>3</sub>N<sub>4</sub> with monochromatic light irradiations. Note: 5.0 mg catalyst and 20.0 mL deionized water with 0.1 M AA as a sacrifice reagent. (b) Wavelength-dependent photocatalytic H<sub>2</sub> evolution rate and DRS spectrum of 2.5-TBTA/g-C<sub>3</sub>N<sub>4</sub>.

**Table S2.** Comparison of the performance of photocatalytic H<sub>2</sub> evolution rate of organic semiconductor/g-C<sub>3</sub>N<sub>4</sub> hybrids with Pt as co-catalysts.

Photocatalyst	Co-catalyst	Sacrificial agent	Irradiation condition	Reaction rate (H <sub>2</sub> evolution)	Ref.
2.5-TBTA/g-C <sub>3</sub> N <sub>4</sub>	3.0 wt% Pt	AA	$\lambda \geq 420$ nm (300 W Xe lamp)	26.04 mmol/g/h	<i>This work</i>
Flu-DFBA/g-C <sub>3</sub> N <sub>4</sub>	1.0 wt% Pt	TEOA	$\lambda \geq 420$ nm (300 W Xe lamp)	14.85 mmol/g/h	7
P <sub>3</sub> /g-C <sub>3</sub> N <sub>4</sub>	1.0 wt% Pt	TEOA	$\lambda \geq 420$ nm (300 W Xe lamp)	13.00 mmol/g/h	8
PFBT/g-C <sub>3</sub> N <sub>4</sub>	1.0 wt% Pt	TEOA	$\lambda \geq 420$ nm (300 W Xe lamp)	0.72 mmol/g/h	9
P3HT/g-C <sub>3</sub> N <sub>4</sub>	1.0 wt% Pt	AA	$\lambda \geq 500$ nm (300 W Xe lamp)	3.05 mmol/h	10
PPy/ g-C <sub>3</sub> N <sub>4</sub>	3.0 wt% Pt	without	$\lambda \geq 400$ nm (300 W Xe lamp)	0.39 mmol (25 h)	11
Pt/C <sub>3</sub> N <sub>4</sub> -P3HF	1.0 wt% Pt	Na <sub>2</sub> S-Na <sub>2</sub> SO <sub>3</sub>	$\lambda \geq 400$ nm (300 W Xe lamp)	0.56 mmol/h	12

**Table S3.** Comparison of the performance of photocatalytic H<sub>2</sub> evolution rate of g-C<sub>3</sub>N<sub>4</sub>-based heterostructured photocatalysts without noble metal as co-catalyst.

Photocatalyst	Co-catalyst	Sacrificial agent	Irradiation condition	Reaction rate (H <sub>2</sub> evolution)	Ref.
2.5-TBTA/g-C <sub>3</sub> N <sub>4</sub>	none	AA	$\lambda \geq 420$ nm (300 W Xe lamp)	11.73 mmol/g/h	<i>This work</i>
Flu-DFBA/g-C <sub>3</sub> N <sub>4</sub>	none	TEOA	$\lambda \geq 420$ nm (300 W Xe lamp)	2.73 mmol/g/h	1
MG@hm-C (CN) <sub>3</sub>	none	TEOA	300 W Xe lamp	1.01 mmol/g/h	13
CNPS-NH <sub>2</sub>	3.0 wt% Ni	TEOA	$\lambda \geq 420$ nm (300 W Xe lamp)	1.23 mmol/g/h	14
Phosphorene/ g-C <sub>3</sub> N <sub>4</sub>	Phosphorene	lactic acid	$\lambda \geq 400$ nm (300 W Xe lamp)	0.57 mmol/g/h	15
C <sub>3</sub> N <sub>4</sub> /(FeTPP) <sub>2</sub> O	none	TEOA	$\lambda \geq 420$ nm (300 W Xe lamp)	0.18 mmol/g/h	16
Black phosphorous/ g-C <sub>3</sub> N <sub>4</sub>	none	Methanol	$\lambda \geq 420$ nm (300 W Xe lamp)	0.43 mmol/g/h	17
C,N-TiO <sub>2</sub> /g-C <sub>3</sub> N <sub>4</sub>	none	TEOA	$\lambda \geq 400$ nm (300 W Xe lamp)	0.039 mmol/g/h	18



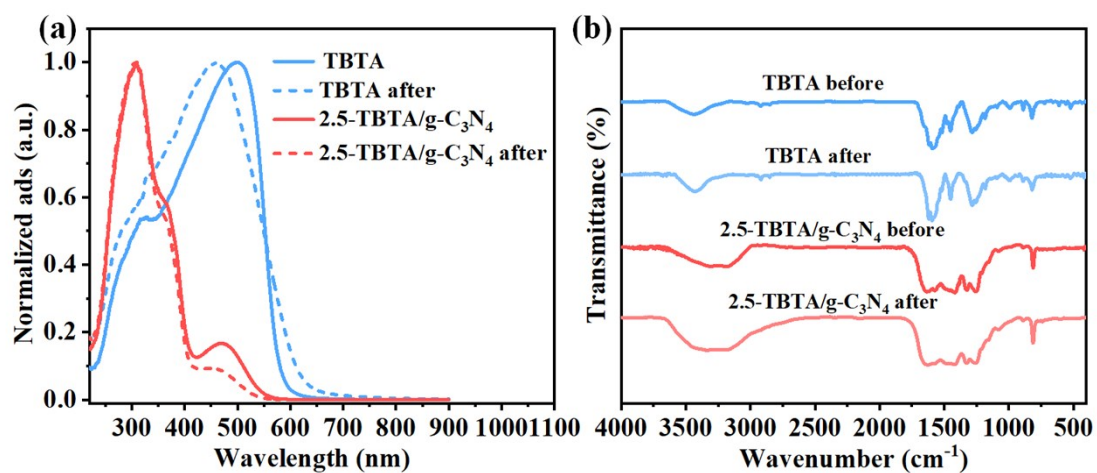


**Fig. S9** Comparison of (a) DRS (b) IR before and after H<sub>2</sub> production process.

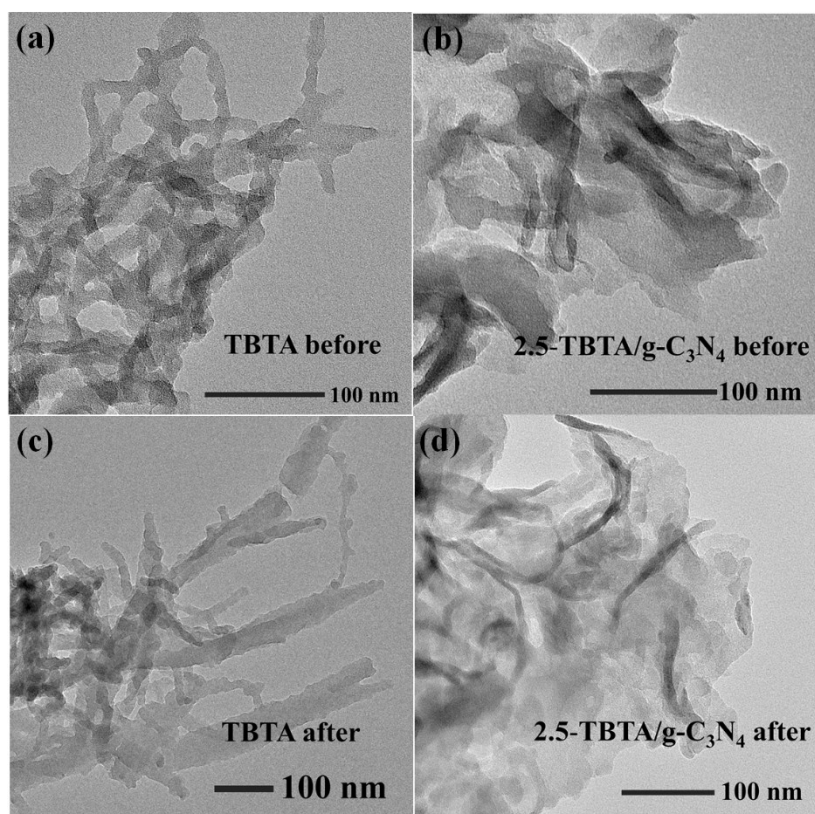


**Fig. S10** Comparison of TEM images before and after H<sub>2</sub> production process.



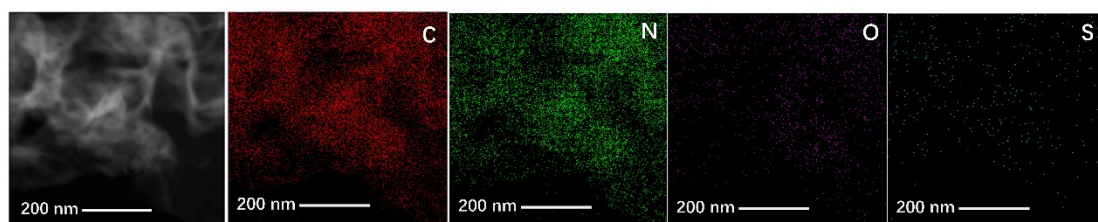


**Fig. S11** HAADF-STEM image and elemental mappings of 2.5-TBTA/g-C<sub>3</sub>N<sub>4</sub> after H<sub>2</sub> production process.

**Table S4.** PL Decay parameters.

Samples	Lifetime, $\tau$ (ns)	Pre-exponential factors, A%	Average lifetime, $\tau$ (ns)
TBTA	0.58	70.60	1.12
	2.43	29.40	
2.5-TBTA/g-C <sub>3</sub> N <sub>4</sub>	0.24	74.27	0.75
	2.23	25.73	

## Notes and references

- 1 C.-C. Li, M.-Y. Gao, X.-J. Sun, H.-L. Tang, H. Dong and F.-M. Zhang, *Appl. Catal. B: Environ.*, 2020, **266**, 118586.
- 2 W. L. Fu, J. M. Wang, S. Y. Zhou, R. J. Li and T. Y. Peng, *ACS Appl. Nano Mater.*, 2018, **6**, 2923-2933.
- 3 J. M. Wang, Y. Zheng, T. Y. Peng, J. Zhang, R. J. Li, *ACS Sustainable Chem. Eng.*, 2017, **5**, 7549-7556.
- 4 J. P. Perdew, K. Burke and M. Ernzerhof, *Phys. Rev. Lett.*, 1996, **77**, 3865.
- 5 G. Kresse and D. Joubert, *Phys. Rev. B*, 1999, **59**, 1758.
- 6 D. J. Chadi, *Phys. Rev. B*, 1977, **16**, 5188-5192.
- 7 H. N. Ye, Z. Q. Wang, F. T. Yu, S. C. Zhang, K. Y. Kong, X. Q. Gong, J. L. Hua and H. Tian, *Appl. Catal. B: Environ*, 2020, **267**, 118577.
- 8 F. T. Yu, Z. Q. Wang, S. C. Zhang, H. N. Ye, K. Y. Kong, X. Y. Gong, J. L. Hua and H. Tian, *Adv. Funct. Mater.*, 2018, 1804512.
- 9 J. Chen, C.-L. Dong, D. M. Zhao, Y.-C. Huang, X. X. Wang, L. Samad, D. Lianna, M. Shearer, S. H. Shen and L. J. Guo, *Adv. Mater.*, 2017, **29**, 1606198.
- 10 X. H. Zhang, B. S. Peng, S. Zhang and T. Y. Peng, *ACS Sustainable Chem. Eng.*, 2015, **3**, 1501-1509.
- 11 Y. Sui, J. H. Liu, Y. W. Zhang, X. K. Tian and W. Chen, *Nanoscale*, 2013, **5**, 9150.
- 12 H. Yan and Y. Huang, *Chem. Commun.*, 2011, **47**, 4168-4170.
- 13 G. Zhou, Y. Shan, Y. Y. Hu, X. Y. Xu, L. Long, J. L. Zhang, J. Dai, J. H. Guo, J. C. Shen, S. Li, L. Z. Liu and X. L. Wu, *Nat. Commun.*, 2018, **9**, 3366.

- 14 N. N. Meng, J. Ren, Y. Liu, Y. Huang, T. Petit and B. Zhang, *Energy Environ. Sci.*, 2018, **11**, 566-571.
- 15 J. R. Ran, W. Guo, H. L. Wang, B. C. Zhu, J. G. Yu and S.-Z. Qiao, *Adv. Mater.*, 2018, **30**, 1800128.
- 16 D. H. Wang, J. N. Pan, H. H. Li, J. J. Liu, Y. B. Wang, L. T. Kang and J. N. Yao, *J. Mater. Chem. A*, 2016, **4**, 290-296.
- 17 M. S. Zhu, S. Kim, L. Mao, M. Fujitsuka, J. Y. Zhang, X. C. Wang and T. Majima, *J. Am. Chem. Soc.*, 2017, **139**, 13234-13242.
- 18 W. Chen, T.-Y. Liu, T. Huang, X.-H. Liu, G.-R. Duan, X.-J. Yang and S.-M. Chen, *RSC Adv.*, 2015, **5**, 101214-101220.